*Korean J. Chem. Eng.*, **16**(5), 640-645 (1999)

# Simulation of the 200 MWe Tonghae Thermal Power Plant Circulating Fluidized Bed Combustor by using IEA-CFBC Model

**Jong-Min Lee† and Jae-Sung Kim**

Advanced Power Generation & Combustion Group, Power Generation Laboratory,
Korea Electric Power Research Institute, Korea Electric Power Corporation,
103-16 Munji-dong, Yusung-gu, Taejon 305-380, Korea
(*Received 2 April 1999 • accepted 30 May 1999*)

**Abstract**–The 200 MWe Tonghae thermal power plant CFB boiler (2-units) is the largest boiler to fire a Korean anthracite coal for generation of electric power. The #1 unit CFB has been operated commercially since October 1998, and the #2 unit CFB, which will begin commercial operation in October 1999, is currently under construction. However, there is little operational data of the large CFB combustor firing anthracite coal, so it is necessary to predict the performance of the CFB combustor with variation of the operation conditions. Therefore, in this study, the simulation of the Tonghae CFB has been carried out to predict the performance with various nominal rates, coal particle size distribution and operating conditions. The simulation results with various loads could be fitted well to the design values at the given operation conditions. At the various operation conditions, the simulation results could explain the performance of the Tonghae CFBC well.

Key words : CFBC, Tonghae Boiler, IEA-CFBC Model, Korean Anthracite Coal

## INTRODUCTION

The design engineering and construction project of the Tonghae thermal power plant CFBC located in Tonghae, Korea, was begun by Korea Electric Power Company (KEP-CO) to utilize domestic anthracite coal in early 1993. Combustion Engineering, Inc. (ABB-CE) has designed a 200 MWe CFB firing a Korean anthracite fuel. In this project, KOPEC (Korea Power Engineering Company) has served as the project architectural engineering and is responsible for various balances of plant system designs and equipment procurement. Additionally, Hanjung is responsible for the majority of the boiler equipment fabrication and procurement. Erecting the initial CFB steam generator was scheduled for late 1995 and initial firing and steam blows were scheduled for late 1997. In late 1998, commercial operation was achieved.

The Tonghae CFB consists of a rectangular furnace, three cyclones, loopseals and fluidized bed heat exchangers (FBHEs) and a fluidized bed ash cooler (FBAC). The furnace (aspect ratio of more than 2 : 1), especially, is designed to fire an indigenous Korean fuel that is low grade and reactivity anthracite, which is different from other CFBCs using subbituminous coal [Maitland and Schaker, 1997].

In this study, the Tonghae CFBC was simulated to predict the performance with various operating conditions by using the IEA-CFBC model which was developed by the members of the mathematical modeling group of the International Energy Agency (IEA) [Hannes, 1993; Hannes et al., 1995; Hannes, 1996]. This model describes the overall process in the furnace, including gas and solid flows, development of the particle size distribution, coal conversion, homogeneous and catalytic gas reactions as well as heat transfer to membrane walls and to tube bundles. Therefore, the simulation of the Tonghae CFBC has been carried out to predict the performance CFBC with coal particle size distribution, operating conditions and various nominal rates.

†To whom correspondence should be addressed.
E-mail : jmlee@kepri.re.kr

## IEA-CFBC MODEL FEATURES

An overall CFBC model consists of several fields of mechanical, chemical and thermal processes, which are dependent on each other during the CFBC process. In the following, an overview of the process is given.

### 1. Fluidization Pattern of Solid Flow

The mechanical gas/solid interactions in a CFB lead to an inhomogeneous flow structure in a riser. In the bottom, a dense bed can be observed. Above, a transition zone exists going over into a transport zone. As boundary conditions for this flow structure the emulsion density and the bubble fraction in the dense bed must be calculated as well as the density of the transport zone at the top. This is done using empirical or half-empirical equations published in the literature. The shape of the transition zone in-between is calculated empirically [Wen and Chen, 1982; Wirth, 1988]. Furthermore, the split between a lean core zone and a denser annulus is considered. Since the bed material is not monosized, size distribution is taken into account. The flow patterns are calculated individually for each size class, assuming a monosize distribution in the riser, and the individual results are superposed according to the mass fractions of the size classes.

### 2. Development of Particle Size Distribution

Different materials are fed into the riser as coal, limestone and sometimes sand. Fine bed material which is elutriated and

not captured by the cyclone gets lost in the filters. Coarse ashes are discharged from the bottom beds. This keeps the bed material fine enough to circulate. Particles, especially coal, fragmentate due to the thermal shock during its feeding into the combustor. Mechanical stresses and uneven surface structures caused by chemical reactions lead to an attrition of fine particles from bigger particles which in turn shrink in diameter. The combination of these effects can establish a size distribution in the boiler which is much different from the coal initially fed.

**3. Gas Flow**

According to flow pattern calculations the gas is split into core, annulus and bubble flow which are balanced parallel and connected by gas exchange rate, calculated by dispersion approaches from literature.

**4. Coal Conversion**

Once into the combustor, the coal particles are heated up and dried causing the coal to fragmentate as the evaporating water blasts the particle. Once dried, the particles are heated up further and release volatiles, leaving a residue of carbon and ash, the char. These effects can happen in parallel to one another. This is considered by calculating the transient temperature profiles in the particles. The char combustion is now the real gas-solid reaction. Diffusion and reaction equilibrium, heat generation, and particle release determine the char combustion rate and the particle temperature. The char concentration in the bed is balanced in turn with the oxygen concentration in the gas phase. The two concentrations are balanced in a surrounding iteration loop.

**5. Homogeneous and Heterogeneous Gas Reactions**

Homogeneous gas reactions take place without any catalytic support of solid materials. They can be balanced straight in the gas phase. However, the effect of incomplete radial mixing of the gas cannot be modeled in a one-dimensional approximation [Korbee, 1995].

**6. Heat Transfer**

The main heat extraction appears to membrane tube walls in the upper section of the riser, external heat exchangers or ash coolers. The major part of the heat transfer is caused by particle convection and radiation. The calculation of the particle convection is very sensitive towards the fluidization pattern since this determines the particle wall collisions necessary for intense heat transfer. The radiation must be applied considering the down flowing particle layer at the wall, which may be optically dense, reducing the radiative part [Wirth, 1995; Grace et al., 1997].

The models are applied as submodels in the IEA-code and are called and initialized by the main balancing and administration routines to combine the different approaches and iterate the necessary cross dependencies until equilibrium is reached.

## DESIGN AND OPERATION CONDITIONS OF THE TONGHAE CFBC

The Tonghae thermal power plant CFB boiler is designed to fire an indigenous Korean anthracite fuel by Combustion Engineering, Inc. [ABB-CE, 1994]. The Tonghae CFBC, which is shown in Fig. 1, consists of feeding parts of coal and limestone, primary air (PA), secondary air (SA) and fluidizing air (FA) supplier, main combustion part (furnace, cyclones, loop-seals, FBHEs and FBAC) and backpass. The combustor (19 m (W)× 7 m(L)×32 m(H)) has a rectangular footprint and is significantly wider than it is deep, incorporating an aspect ratio of more than 2 : 1. The lower section (to about 7 m from distributor) of the combustor is tapered and is covered with an erosion-resistant plastic refractory material manufactured by Chosun Refractory Company. As all the fuel feed points are along the combustor front wall, the rectangular geometry was chosen to allow for good fuel mixing. Fuel is introduced into the combustor at six locations along the front wall. Limestone is injected with the fuel in the fuel feed chutes and it is also introduced in two injection ports along the rear wall.

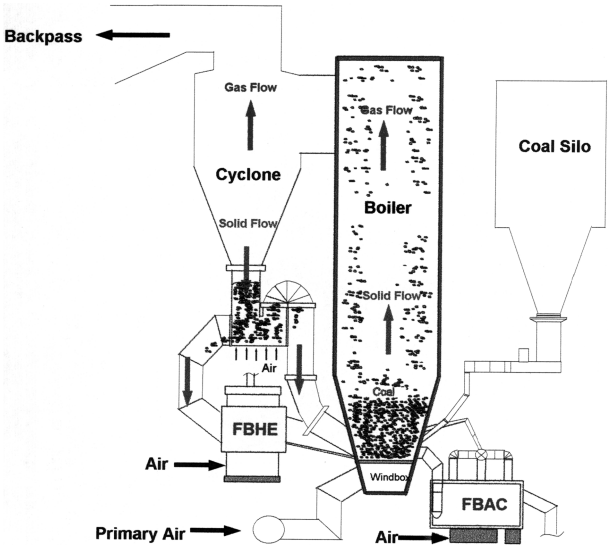


**Fig. 1. Schematic diagram of the Tonghae CFB boiler.**

Primary air (PA) is introduced to the combustor via the fluidization grate. The grate is comprised of T-style fluidizing nozzles patented by ABB-CE. The T-style fluidizing nozzles include relatively large openings to reduce the potential of plugging associated with many nozzle designs, while maintaining a pressure drop to preclude backsifting. The T-style fluidizing nozzles are employed in the fluid bed heat exchangers as well as in the seal pots. Secondary air (SA) is introduced at the lower combustor along the front and rear walls and into the four start-up burners. Bottom ash is removed from the bottom of the combustor via two ash control valves (ACV), and is introduced into a fluidized bed ash cooler (FBAC) which contains the economizer and cooling water heat transfer surface. Heated fluidizing air is returned from the FBAC vents into the combustor at four locations along the front wall.

Three refractory-lined steel plate cyclone separators are fitted up to receive the flue gas and solids mixture from the combustor. The loopseals serve to create a pressure seal from positive pressure in the combustor to the negative pressure in the cyclone. This pressure seal prevents the flow of material back up the cyclone from the bottom of the combustor. The loopseal (or sealpot) is a compact, low velocity multi chamber fluidization grate. On the Tonghae CFBC unit, the boiler turndown requirement, coupled with the difficult to burn anthracite fuel, resulted

**Table 1. Input variables for Tonghae CFBC**

| # | H (m) | W (m) | L (m) | Addition air ($m^3$/s) | | | | | | Taper* | Wall ratio** |
|---|---|---|---|---|---|---|---|---|---|---|---|
| | | | | BMCR | MGR | 100%NR | 75%NR | 50%NR | 30%NR | | |
| 1 | 0.0 | 19.05 | 3.35 | 87.22 | 87.22 | 87.22 | 76.3 | 65.58 | 68.34 | 1 | 1 |
| 2 | 0.43 | 19.05 | 3.58 | 14.6 | 14.01 | 10.26 | 4.4 | 4.4 | 4.4 | 1 | 1 |
| 3 | 1.37 | 19.05 | 4.09 | 0.93 | 0.93 | 0.93 | 0.93 | 0.93 | 0.93 | 1 | 1 |
| 4 | 1.70 | 19.05 | 4.26 | 9.14 | 9.14 | 9.14 | 9.14 | 9.14 | 7.34 | 1 | 1 |
| 5 | 2.44 | 19.05 | 4.66 | 22.19 | 21.75 | 18.94 | 14.54 | 14.54 | 14.54 | 1 | 1 |
| 6 | 4.48 | 19.05 | 5.75 | 32.86 | 31.52 | 23.09 | 9.9 | 9.9 | 9.9 | 1 | 1 |
| 7 | 28.53 | 19.05 | 7.09 | 0 | 0 | 0 | 0 | 0 | 0 | 0 | 1 |
| 8 | 32.90 | 19.05 | 7.09 | 0 | 0 | 0 | 0 | 0 | 0 | 0 | 1 |
| 9 | Coal (kg/s) | | | 30.1 | 29.7 | 27.3 | 20.7 | 14.5 | 7.9 | | |
| 10 | Lime (kg/s) | | | 0.92 | 0.91 | 0.83 | 0.63 | 0.44 | 0.38 | | |
| 11 | Average bed T (°C) | | | 900 | 900 | 900 | 900 | 820 | 700 | | |

BMCR: Boiler Maximum Continued Rate, MGR: Maximum Guaranteed Rate, NR: Nominal Rate
#1: Primary air, #2: Secondary air (4 points), #3: Feeder (coal and limestone) transport air, #4: Loopseal+FBHE returned air, #5: Secondary air (3 points), #6: Secondary air (9 points), #7: Exit, #8: Top of combustor, #9, 10: coal and limestone feed rate, *Taper: Tapered or not, yes=1, no=0, **Wall ratio: [membrane wall area]/[wall area]

in external fluid bed heat exchangers (FBHEs). At each of the three loopseals, a stream of solids materials is diverted and introduced into an FBHE. The FBHEs are bubbling beds containing natural circulation evaporative, superheat and reheat heat transfer surface. As the solids from the loopseals flow over and through the FBHE heat transfer surfaces, the ash is cooled and then returned to the combustor. By placing superheat and reheat heat transfer surface in separate FBHEs into which solids can be introduced in a controlled fashion, optimum turndown control is accomplished. Independently controllable solid flows into the superheater and reheater FBHEs allows one to make up marginal heat duties without altering backpass performance or requiring spray [Maitland and Schaker, 1997].

In the Tonghae CFBC, indigenous Korean anthracite coal is used as fuel, which contains 39% ash, 4% VM, 53.7% FC and 3.3% moisture. The coal contains low S (0.6%) and N (0.2%) and its heating value and the combustion reactivity are very low as previously reported by Shun et al. [1996]. The fraction of coal in the range of 0.1-3 mm is over 95% on the design basis. Limestone used in the Tonghae CFBC contains 90% of $CaCO_3$ and 4.2% of $MgCO_3$ and the fraction of particles smaller than 1 mm is 100% (<0.7 mm-95%, <0.5 mm-90%).

In this study, to predict the performance of the Tonghae CFBC, the simulation of the CFBC with operation conditions (nominal rate, particle size distribution, gas velocity, PA/SA ratio, bed pressure and excess air ratio) has been carried out by using the IEA-CFBC model. The operation condition with variation of nominal rates for simulation is shown in Table 1.

## RESULTS AND DISCUSSION

Simulation result of solid hold up along the combustor height with variation of load (30-100% NR), the conditions of which are based on the design values of operations, is shown in Fig. 2. As the load, but 50% NR, increases, solid hold-up in the dense phase decreases (0.135-0.1) due to the increase of PA flow and solid feed rate and due to the variation of total pressure of the bed. The solid fraction and the bed height in dense phase have the highest value at 50% NR under the minimum PA flow. Whereas, the solid hold up (about 0.008) in lean phase does not change appreciably with variation of nominal rate. The particle size distributions in overflow, bed content, recirculation and bagfilter are that the fine particles are more included with decreasing load because of the amount of PA and SA and the operating temperature affecting gas velocity. Also, the circulation rate increases about 60% as the load increases from 30% to 100% NR, and the recirculation ratio (recirculated solid /feed) is about 41 at 100% NR. The total gas flow rate (mol/s) with the bed height increases up to place of secondary air installed, and does not change appreciably above the place. This

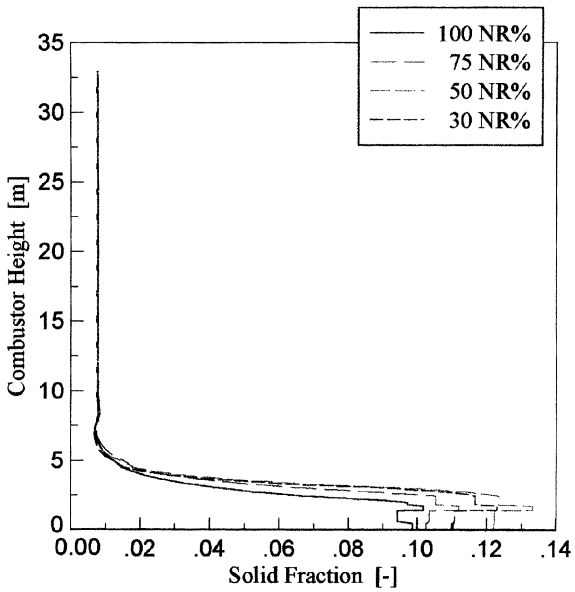


**Fig. 2. Solid fraction vs. combustor height with variation of loads.**

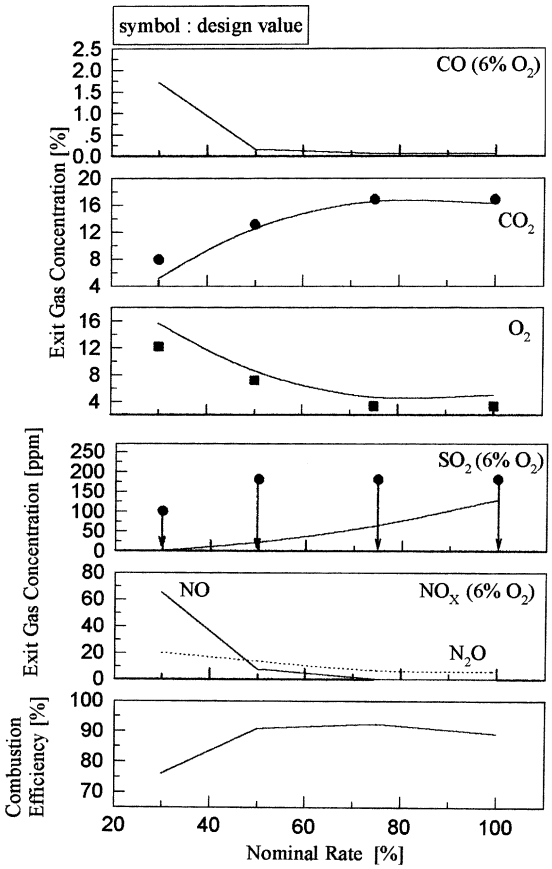


**Fig. 3. Gas composition and combustion efficiency with variation of loads.**

implies that a mole of reacted gas is almost equal to that of produced gas; the main reaction affecting the total gas flow rate is $C+O_2(g)=CO_2(g)$. Also, the gas flow rate almost increases with increasing load.

The exit-gas and the pollutant concentrations are shown in Fig. 3. As can be seen, the CO and $O_2$ yields decrease at 50% NR due to the increase of the operating temperature resulting in enhancement of combustion reactivity. For the same reason, the yield of $CO_2$ increases with load. The pollutants such as $SO_x$ and $NO_x$ are predicted lower emissions, respectively, since the used coal contains a little sulfur and nitrogen compound relatively. The emission of $SO_x$ increases and the emission of $NO_x$ decreases, since the bed temperature and the available oxygen have an influence on the pollutant emissions. The high availability of oxygen leads to an increase of $NO_x$ compound, and the increasing temperature leads to a decrease of $NO_x$ and to an increase of $SO_x$ compounds, which are also affected by combustion efficiency. The model calculations predict well the design value of operation (symbol) as shown in Fig. 3.

With particle size distributions (#1-PSD: coarser than design PSD, #2-PSD: finer than design PSD, #3-PSD: including much coarse and fine particles, shown in Fig. 4), the solid hold up and the bed pressure difference of #1-PSD in the dense phase are the highest. Whereas in the lean phase they are the lowest, since coarse particles are more included in #1-PSD. If fine particles are more included (#2-PSD), the solid fraction and the

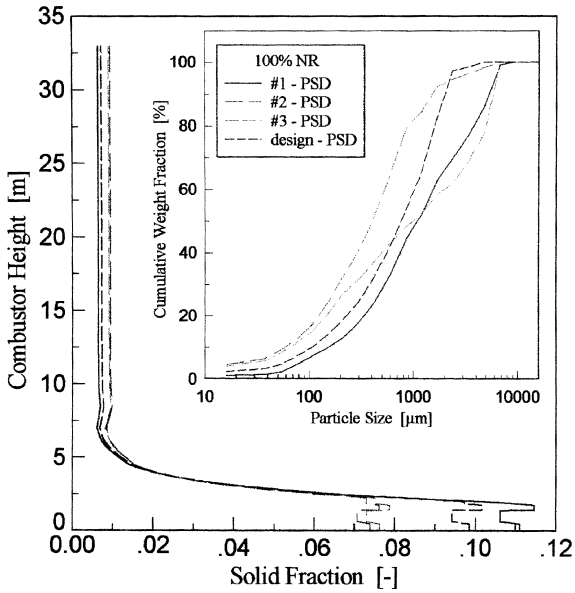


**Fig. 4. Solid fraction vs. combustor height with variation of PSD.**

bed pressure along the bed height have the reverse tendency as compared with those of #1-PSD. The particle distribution containing finer and coarser than that of design value (#3-PSD) has almost same tendency of #2-PSD. However the recirculation rate increases with fine particles more included.

The temperature and the gas flow rate profiles in the combustor with variation of PSD do not change appreciably, as shown in Fig. 5. During the initial firing period in the Tonghae CFBC, the PSD more containing more fine particles leads to an increase of the temperature of the upper part of the combustor and the sealpots, which results in the formation of clinker in the sealpots. However, from the temperature profile in the combustor, if steady-state operation were achieved, the temperature of the bed and sealpots would be stable and get to be low.

The exit-gas and the pollutant concentrations with PSD are

**Table 2. Coal size distributions used for simulation**

| Size distribution (mm) | Design PSD* (wt%) | #1 PSD (wt%) | #2 PSD (wt%) | #3 PSD (wt%) |
|---|---|---|---|---|
| > 9.5 | 0 | 1.0 | 0 | 0 |
| 5.6-9.5 | 0 | 14.4 | 5.0 | 24.4 |
| 4.75-5.6 | 1.0 | 5.1 | 1.2 | 5.1 |
| 2.8-4.75 | 2.0 | 12.3 | 2.9 | 11.5 |
| 2-2.8 | 16.0 | 7.2 | 2.4 | 4.0 |
| 1.0-2.0 | 31.0 | 20.0 | 14.0 | 11.0 |
| 0.6-1.0 | 16.0 | 14.6 | 20.0 | 6.0 |
| 0.25-0.6 | 17.0 | 14.6 | 26.0 | 12.0 |
| 0.1-0.25 | 10.0 | 5.8 | 17.9 | 13.6 |
| 0.075-0.1 | 2.0 | 3.0 | 3.1 | 2.4 |
| < 0.075 | 5.0 | 2.0 | 11.0 | 10.0 |

*PSD : Particle Size Distribution
#1,2,3-PSD : Sampling from coal feeder of the Tonghae CFB boiler.

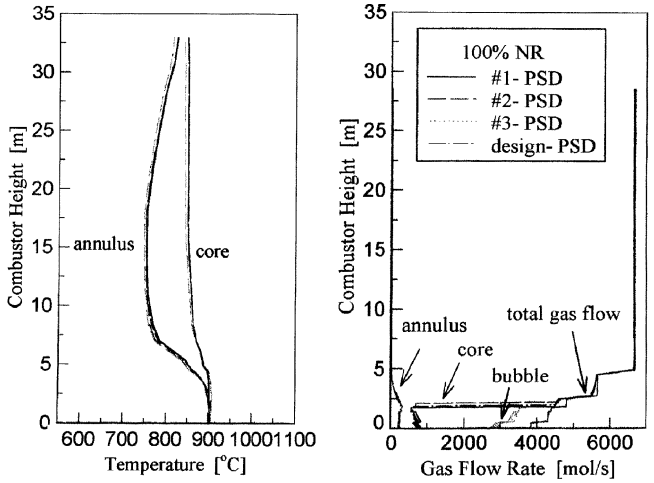


**Fig. 5. Temperature and gas flow rate profiles in the combustor with variation of PSD.**

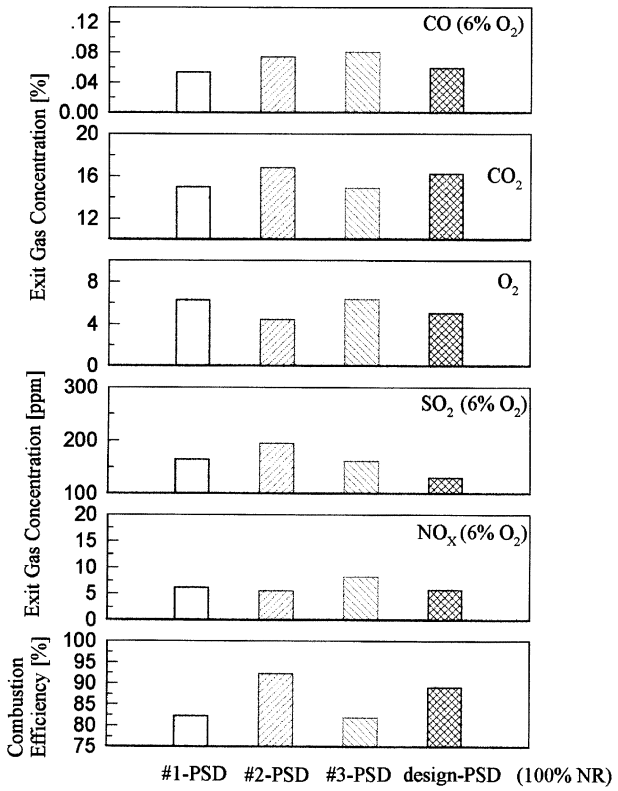


**Fig. 6. Gas composition and combustion efficiency with variation of PSD.**

shown in Fig. 6. The emission of CO in #3 and #2-PSD is higher than that in designed-PSD, and the emission of pollutants ($SO_x$ and $NO_x$) in design-PSD is the lowest. From this fact, the emission of CO is mainly influenced by fine particles, which results in an increase of cyclone inlet temperature due to remixing of CO/unreacted carbon and $O_2$. Whereas the emission of pollutants may be influenced by other operation parameters as well as fine and coarse particles. For the combustion efficiency, the coarse particles lead to a decrease of the efficiency due to more discharge of unreacted coarse particles from the combustor.

With variation of the split ratio of primary to secondary air

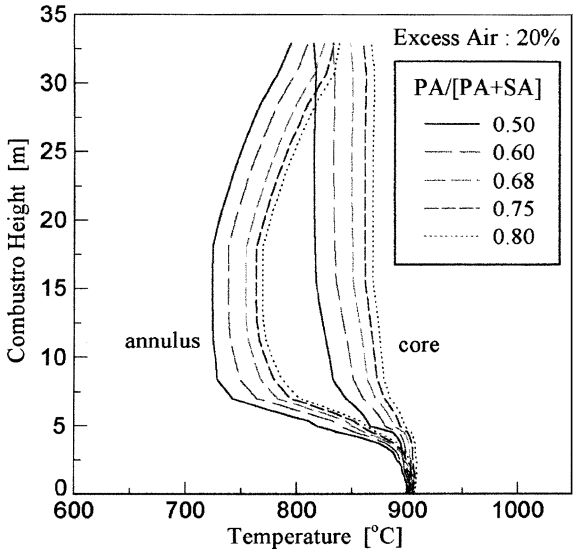


**Fig. 7. Temperature profile in the combustor with PA/(PA+SA) ratio.**

(PA/PA+SA), the temperature profile (core and annulus) in the combustor is shown in Fig. 7. The temperature difference between the dense bed and the freeboard region decreases with increasing the split ratio (PA/PA+SA) since the solid fraction that is producing and transferring heat in the combustor is different with the ratio. The solid fraction in the dense phase decreases from 0.163 to 0.74 with increasing the ratio (PA/PA+SA) and that in the lean phase increases. Also, the circulation rate increases with increasing the ratio. From this fact, the increasing PA flow leads to an increase of the temperature of the freeboard and the circulation rate.

The particle sizes of the overflow and bed contents are much finer, whereas those of the recirculation and bagfilter contents are coarser as the ratio increases, because the elutriated particles are much coarser with increasing PA flow (shown in Fig 8). The combustion efficiency somewhat increases. The opera-

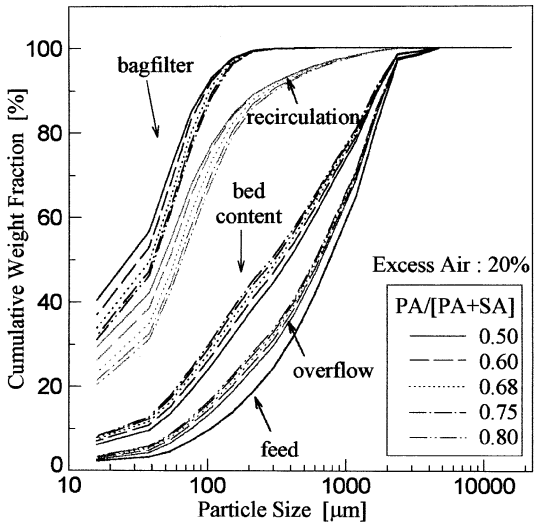


**Fig. 8. Particle size distribution with variation of PA/(PA+SA) ratio.**

tion temperature in a real plant is required for simulation, since the average temperature of the combustor is an input parameter in this model. Though the operation temperature in the Tonghae CFBC was not measured, the effect of temperature on the performance of CFBC was also determined. The variation of temperature of the combustor leads to variation of the gas emission and the combustion efficiency. As the temperature increases from 800 to 1,000 °C, the emissions of CO, $O_2$ and $N_2O$ decrease and the emissions of $SO_2$ and $CO_2$ and the combustion efficiency increase due to enhancement of combustion reaction. However, little NO is emitted since the coal contains only 0.2% N.

As the bed pressure that means the inventory of the bed increases from 4,900 to 14,700 Pa, the solid fraction is almost same at about 0.1 in the dense phase, but in the lean phase the solid hold up increases from 0.008 to 0.02. Also, the increasing bed pressure leads to an increase in the bed height (about 1.5-7.5 m) and the recirculation rate as previously reported by Choi et al. [1995]. In the case of higher bed pressure, the temperatures in the dense and lean phase are somewhat higher, and the temperature in the transition region is much higher, resulting in a flat temperature profile along the combustor height with increasing bed pressure. The increasing bed inventory also leads to decreases of the emission of $SO_x$ and to increases of the combustion efficiency since the solid residence time in the bed is longer at the given operation condition.

## CONCLUSIONS

The simulation of the Tonghae CFBC by using IEA-CFBC model has been carried out with various operation conditions and particle size distributions. The simulation results with various loads could be fitted well to the design values at given operation conditions. The temperature of the combustor with variation of PSD does not change appreciably, in spite of fine particles increasing the temperature of the upper part of the combustor and the sealpots during the initial firing step. Therefore, the temperature of the bed and sealpots would be stable if the steady-state operation was achieved. Also, for the various operation conditions, the simulation results could explain well the performance of the Tonghae CFB

## REFERENCES

ABB-CE, "General Design Conditions," A Contract of Tonghae CFB Boiler, **2**, 171 (1994).

Grace, J. R., Avidan, A. A. and Knowlton, T. M., "Circulating Fluidized Beds," Blackie Academic & Professional, London (1997).

Choi, J. H., Park, J. H., Choung, W. M., Kang, Y. and Kim, S. D., "Hydrodynamic Characteristics of Fine Particles in the Riser and Standpipe of a Circulating Fluidized Bed," *Korean J. Chem. Eng.*, **12**, 141 (1995).

Hannes, J. P., "Mathematical Modeling of CFBC: An Overview Modular Programming Frame Using a 1.5-Dimensional Riser Model," Proc. of the 12th Int. Conf. on Fluidized Bed Combustion, 455 (1993).

Hannes, J. P., "Mathematical Modeling of Circulating Fluidized Bed Combustion," Ph.D. Thesis, RWTH Aachen, Germany (1996).

Hannes, J. P., Renz, U. and Bleek, C. M., "The IEA Model for Circulating Fluidized Bed Combustion," Proc. of the 13th Int. Conf. on Fluidized Bed Combustion, 287 (1995).

Korbee, R., "Regenerative Desulfurization in an Interconnected Fluidized Bed System," Ph. D. Thesis, Delft, The Netherlands (1995).

Maitland, J. and Schaker, Y., "Design of the 200 MWe Tonghae Power Plant Circulating Fluidized Bed Steam Generator," Proc. of the 14th Int. Conf. on Fluidized Bed Combustion, 191 (1997).

Shun, D., Bae, D. H., Hee, K., Son, J. E., Kang, Y., Wee, Y. H., Lee, J. S. and Ji, P. S., "Circulating Fluidized Bed Combustion of Korean Anthracite," *HWAHAK KONGHAK*, **34**, 321 (1996).

Wen, Y. C. and Chen, L. H., "Fluidized Bed Phenomena: Elutriation and Entrainment," *AIChE Journal*, **6**, 117 (1982).

Wirth, K. E., "Axial Pressure Profile in Circulating Fluidized Beds," *Chem. Eng. Technol.*, **11**, 11 (1988).

Wirth, K. E., "Heat Transfer in Circulating Fluidized Beds," *Chem. Eng. Sci*., **50**, 2137 (1995).